

# Studies of diffusion in polymers by ultraviolet microscopy: 2. Diffusion of atactic fractions in isotactic polypropylene

N. C. Billingham, P. D. Calvert and A. Uzuner

School of Chemistry and Molecular Sciences, University of Sussex, Brighton BN1 9QJ, UK

(Received 4 May 1989; accepted 16 June 1989)

Ultraviolet (u.v.) absorbing and fluorescent labels have been attached to isotactic and atactic polypropylene by reaction with appropriate sulphonyl azides. The distribution is random and substitution does not affect the crystallization. The labelled polymer can be visualized by u.v. absorption or fluorescence microscopy. By monitoring penetration of isotactic polymer by labelled atactic, the diffusion coefficient of the atactic polymer has been determined over a range of temperatures. The redistribution of atactic polymer during growth of spherulites of isotactic polymer has been studied. Atactic polymer behaves quite differently to small additive molecules. The fibrosity of polypropylene spherulites is associated with rejection of atactic polymer from crystallizing regions. There is significant non-uniformity of atactic content between the spherulite centres and the boundaries.

(Keywords: ultraviolet microscopy; diffusion; atactic polymer; polymer diffusion; crystallization; morphology)

## INTRODUCTION

Diffusion in polymer/polymer systems, both in the melt and in the solid, is an increasingly interesting phenomenon as adhesion of polymers and polymer/polymer blends become more important. Studies of diffusion are rare because of the experimental difficulties of measuring the very low diffusion coefficients. There is also considerable disagreement about the dependence of diffusion coefficients on polymer size. Polymer/polymer diffusion has been reviewed by Tirrell<sup>1</sup>.

The motion of a polymer molecule through an assembly of other polymers is clearly different from the motion of a small molecule. The most recently accepted model for diffusion where both components are polymers is the reptation model of deGennes<sup>2</sup>. This treats the diffusion as analogous to the motion of a flexible snake through a series of fixed obstacles and predicts that the self-diffusion coefficient,  $D$ , will vary as  $M^{-2}$ , where  $M$  is the molecular weight of the diffusing chain.

Tests of the reptation theory for self-diffusion have generally supported the model. Klein<sup>3</sup> estimated self-diffusion rates for short-chain deuterated polyethylenes in polyethylene by infrared (i.r.) microdensitometry and showed the predicted dependence of  $D$  on  $M$ . Mills *et al.*<sup>4</sup> showed a similar dependence for self-diffusion in polystyrene by using  $\alpha$ -scattering to measure diffusion profiles of deuterated polymer, although Kunagi *et al.*<sup>5</sup> found  $D \propto M^{-1}$  for self-diffusion of polystyrene, using tritium-labelled polymer. Gilmore *et al.*<sup>6,7</sup> used energy dispersive analysis by X-rays in an electron microscope to follow interdiffusion of poly(vinyl chloride) and poly( $\epsilon$ -caprolactone) and found  $D \propto M^{-1}$ . In earlier studies of self-diffusion in polystyrene and in poly(*n*-butyl acrylate), Bueche *et al.*<sup>8,9</sup> suggested that the product,  $D\eta$ , of the diffusion coefficient and the melt viscosity is a constant, implying that  $D \propto M^{-3.5}$  for long chains.

In recent publications<sup>10,11</sup> we have shown that the migration of ultraviolet absorbing additives in polyolefins

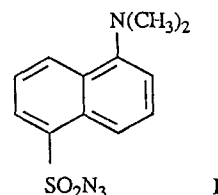
can be monitored very conveniently by microscopy, using u.v. illumination. Calvert and Ryan<sup>12,13</sup> showed that measuring the redistribution of these additives during crystallization of the polymer is a powerful tool for study of morphology.

An important contributor to the behaviour of polypropylene is the atactic fraction, usually present in commercial samples at levels up to 7%. Little is known about the diffusion of atactic polymer or its redistribution during crystallization. We have therefore extended our u.v. microscopy approach to try to study these phenomena.

To generate contrast it is necessary to make either the atactic or the isotactic polymer u.v. absorbing or fluorescent. We have found that this can be achieved via the reaction of an aromatic sulphonyl azide with the polymer<sup>14</sup>:



A very convenient reagent is dansyl azide (1-dimethylamino-5-sulphonyl azide):



in which Ar is the u.v. absorbing and fluorescent dimethylaminonaphthalene group.

## EXPERIMENTAL

### U.v. and fluorescence microscopy

The u.v.-microscope has been described in detail

elsewhere<sup>15</sup>. It is a conventional microscope with the exceptions that the optical system uses quartz lenses and front-surfaced mirrors and illumination uses a Xenon arc lamp. This allows wavelengths down to  $\approx 280$  nm; shorter wavelengths are accessible with a mercury lamp. It is not possible to view a u.v. image with the naked eye. Instead, the images focused on either a 35 mm camera or a television camera, fitted with a u.v.-sensitive Vidicon tube. Quantitative data can be obtained by microdensitometry of photographic negatives. A more convenient method is to use a video waveform monitor, which allows the selection of a single line of the television display and the display of the grey level across that line on an oscilloscope. Calibration experiments have shown that the Beer–Lambert law is obeyed in the microscope so that grey levels can be related directly to absorber concentrations.

For fluorescence, the standard television camera is not sufficiently sensitive and quantitative measurements are made from photographic negatives. The intensity of emission is proportional to the absorbed light. If the absorber concentration is low and the path length short then the absorption follows the Beer–Lambert law and is proportional to the absorber concentration. Scanning the negative with a single-beam microdensitometer gives a signal,  $A$ , related to the density of silver in the negative by  $A = \varphi(\log E + \text{constant})$ , where  $E$  is the total exposure and is equal to the product of the fluorescence intensity and the exposure time. For any given film the value of  $\varphi$  is a constant over a fairly wide range of exposure times, changing at low exposures due to reciprocity failure in the emulsion and at high exposures due to emulsion saturation. To determine  $\varphi$  and to ensure that measurements were made in the linear region, each roll of film was individually calibrated using a series of quenched polymer films containing known concentrations of fluorescer.

For u.v. absorption, the spectral distribution of the illuminating light must be within the absorption envelope of the absorber and this was achieved with appropriate filters. For fluorescence, transmitted u.v. was cut off by a series of barrier filters placed above the sample and chosen to maximize transmission at the fluorescence peak of the dansyl group.

Sectioning and mounting of polymer films for microscopic study have been described previously<sup>11</sup>. Refractive index matching to the mounting fluid is important in fluorescence to avoid artefacts due to scattering.

### Materials

Isotactic polypropylene (IPP) was supplied by ICI PLC as their film-forming grade HF18. Heptane-soluble material was removed by Soxhlet extraction for 24 h before use. The unstabilized polymer was compression moulded at 220°C to films with thicknesses in the range 0.5–1.5 mm which were quenched into ice–water as soon as possible after pressing. This gave films which were morphologically featureless in the microscope under crossed polars.

Atactic polypropylene (APP) was supplied by Hercules Powder Co. and contained some low molecular weight or stereoblock polymer. It was purified by repeated reprecipitation from chloroform solution into methanol to give a product which was wholly atactic as measured by <sup>13</sup>C nuclear magnetic resonance (n.m.r.) and showed no crystallinity in a scanning calorimeter. The number

average molecular weight was determined by viscometry as 8000, using values of  $k = 1.6 \times 10^{-4}$  and  $\alpha = 0.8$  for the Mark–Houwink parameters<sup>16</sup>. Dansyl azide (1-dimethylamino-5-sulphonyl azide) was synthesized by the method of Cantor<sup>14</sup>. A solution of dansyl chloride (Aldrich) in the minimum of ethanol was added dropwise to a saturated aqueous solution of sodium azide at 0°C. After the addition, the solution was stirred overnight at room temperature and the product recovered as dark yellow crystals by addition of a large amount of water. Microanalysis and n.m.r. were consistent with the proposed structure and the i.r. spectrum showed an intense band at  $2130 \text{ cm}^{-1}$ , characteristic of the azide group. The product melts at 42–44°C and decomposes rapidly above 140°C, with evolution of nitrogen.

Labelled atactic polypropylene (LAPP) was prepared by reaction of APP with dansyl azide. APP and dansyl azide were codissolved in chloroform and the solvent was evaporated. The mixture was maintained at 175°C under nitrogen for 2 h, then cooled and redissolved and the polymer was recovered by precipitation into methanol. It was then extracted with methanol under reflux until the extract was no longer fluorescent.

Labelled isotactic polypropylene (LIPP) was prepared by carrying out the binding reaction during compression moulding. A solution of dansyl azide in dichloromethane was mixed with polymer powder and stirred whilst the solvent evaporated. The product was moulded into films as described earlier and the films extracted with methanol until no more fluorescence could be removed.

### Bulk diffusion experiments

For bulk diffusion, samples of IPP film  $3 \text{ cm} \times 4 \text{ cm} \times 0.5 \text{ mm}$  were cut and their surfaces cleaned. A uniform layer of LAPP was deposited on one surface from chloroform solution and then a second layer of film was placed on top to form a sandwich. This was wrapped in aluminium foil and maintained under gentle pressure in a temperature-controlled oven. After the required time diffusion was stopped by immersing the samples in dry ice. The film surfaces were cleaned with cold chloroform to remove adhering polymer and finally microtomed to produce  $10 \mu\text{m}$  sections for microscopy.

### Crystallization studies

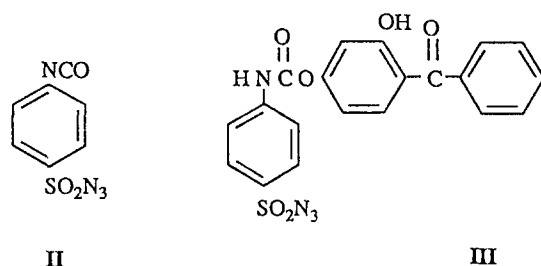
For bulk crystallization studies the required amounts of IPP and APP were codissolved in xylene at 110°C to give a 1% total polymer concentration. This solution was precipitated in cold methanol to yield a powdered polymer. 0.1% of Irganox 1010 antioxidant was added and the mixture was compression moulded at 200°C to form discs. For crystallization in the microscope,  $10 \mu\text{m}$  sections were microtomed from these discs and gently pressed between a slide and a cover slip at 240°C to give an adherent film. During crystallization the hot stage was flooded with nitrogen. Samples crystallized in bulk were small pieces,  $0.5 \times 0.5 \times 1 \text{ cm}$ , cut from the bulk. They were wrapped in aluminium foil, melted at 240°C in a Wood's metal bath then kept in a silicone oil bath at the crystallization temperature before being cooled and microtomed.

## RESULTS

### Fluorescent labelling

The use of a covalently bound absorbing or fluorescing group to allow one polymer to be visualized in a mixture

is a powerful tool for microscopic study<sup>15</sup>. Covalent binding to polyolefins is difficult because of their inherently low reactivity. The sulphonyl azide chemistry, developed by Cantor<sup>14</sup>, is a convenient route for the binding. In our initial experiments, we followed Cantor in synthesizing 4-chlorocarbonylbenzenesulphonylchloride. Reaction of this compound with sodium azide converts the sulphonyl chloride to the sulphonyl azide and the carbonyl chloride to the isocyanate, yielding (II). Reaction of (II) with 2,4-dihydroxybenzophenone produced the strongly u.v.-absorbing product (III).



Preliminary experiments with (III) showed that the urethane linkage did not survive the processing of polypropylene. Accordingly we switched to dansyl azide, which is very easily accessible in a one-step reaction from commercially available dansyl chloride.

The products of reaction of either APP or IPP with dansyl azide were intensely fluorescent, with emission and excitation spectra similar to the unbound dansyl azide. I.r., u.v. and fluorescence spectroscopy all showed that about 50% of the original dansyl compound was bound to the polymer, corresponding to 1 wt% of the polymer in the LAPP and 0.5 wt% in the LIPP. Gel chromatography of APP with a refractive index detector showed essentially identical chromatograms before and after reaction, implying that there is no degradation of the polymer. Gel chromatography of LAPP showed essentially identical chromatograms with a refractive index detector and a u.v.-absorption detector, implying that the absorbing groups are randomly distributed in the polymer. Scanning calorimetry showed that the crystallization of the IPP was unaffected by labelling. The reaction with dansyl azide is thus a very successful way of introducing both u.v. absorption and fluorescence without significant changes in the physical properties of the polymer.

#### Bulk diffusion of APP

The use of u.v. microscopy to measure diffusion coefficients of stabilizing additives in IPP by the 'diffusion-in' method has been described previously<sup>11</sup>. It is based on the measurement of the concentration profile developed from the surface of a polymer in contact with the pure additive and fitting of this profile to the theoretical equation for sorption in a semi-infinite medium<sup>17</sup>:

$$\frac{C_0 - C}{C_0} = \operatorname{erf}\left(\frac{x}{2(Dt)^{1/2}}\right) \quad (1)$$

Diffusion-in experiments were performed using LAPP in exactly the same way, with diffusion allowed to go on for up to 24 h at temperatures in the range 100–135°C. At least two different diffusion times were used at each temperature and the spread of  $D$  values about the mean was typically  $\pm 25\%$ . Figure 1 shows typical profiles at 130°C, showing the good fit between experiment and

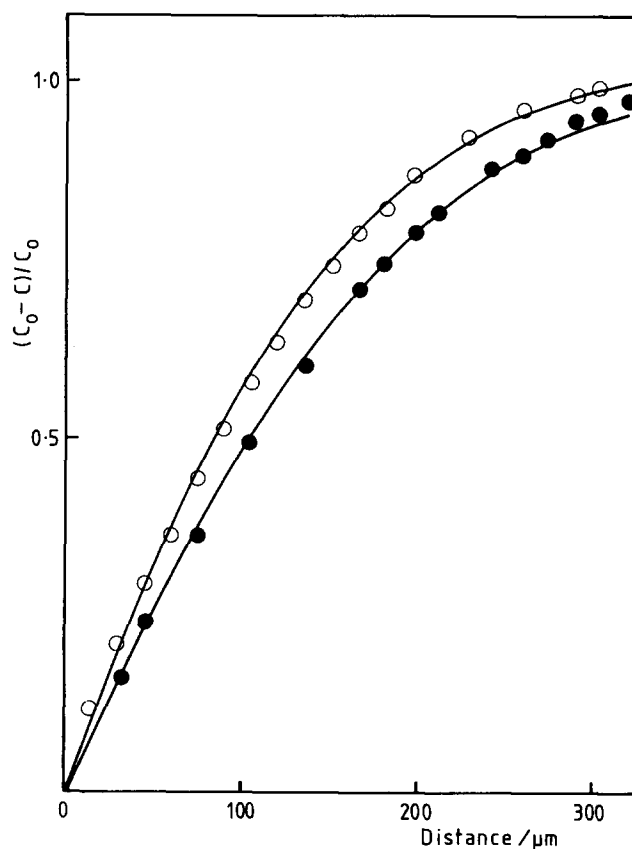


Figure 1 Concentration profiles for diffusion of LAPP in IPP at 130°C: ○, ● experimental data; —, calculated from equation (1). ○, 8 h,  $D=0.298 \mu\text{m}^2 \text{s}^{-1}$ ; ●, 18 h,  $D=0.183 \mu\text{m}^2 \text{s}^{-1}$

Table 1 Diffusion coefficients, for atactic polypropylene in isotactic polymer

Temperature (°C)	$10^9 D$ ( $\text{cm}^2 \text{s}^{-1}$ )
100	0.28
125	1.8
130	2.5
135	3.1

theory. Table 1 shows the measured diffusion coefficients; an Arrhenius plot is a good straight line with a slope corresponding to an activation energy of  $88 \text{ kJ mol}^{-1}$ , independent of temperature over the range studied. This value is comparable with that reported<sup>18</sup> for self-diffusion of polystyrene above  $T_g$  ( $90 \text{ kJ mol}^{-1}$ ) and much larger than that reported<sup>19</sup> for self-diffusion of low molecular weight polyethylene in the melt around 230°C ( $23 \text{ kJ mol}^{-1}$ ).

#### Redistribution of atactic polypropylene

**Distribution in crystallized samples.** Calvert and Ryan<sup>12,13</sup> showed that stabilizing additives are unable to enter the crystal phase of polyolefins. During the initial growth of spherulites, some of the additive is trapped in the amorphous polymer between the lamellae and some is rejected ahead of the growth front. The additives remain sufficiently mobile to equilibrate to a uniform concentration in the amorphous regions after crystallization. U.v. or fluorescence microscopy then showed the distribution of amorphous polymer by staining, much as the biologist uses staining reagents to enhance the contrast of specific cell structures. Here, we have used

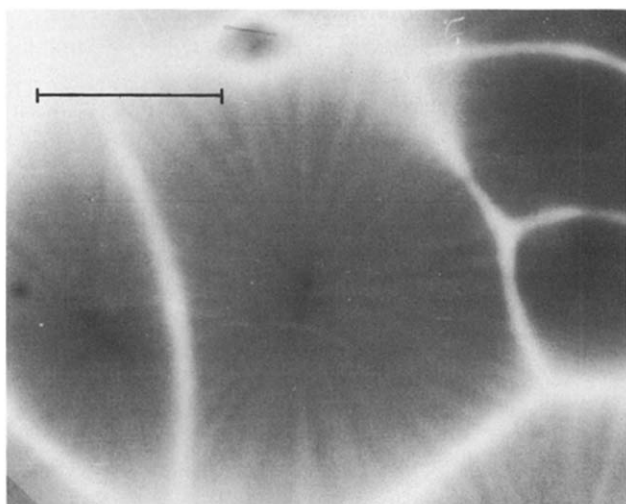


**Figure 2** Fluorescence micrograph of a sample of IPP containing 10% LAPP. Sample was fully crystallized at 140°C and is viewed at room temperature. Scale bar, 200 μm

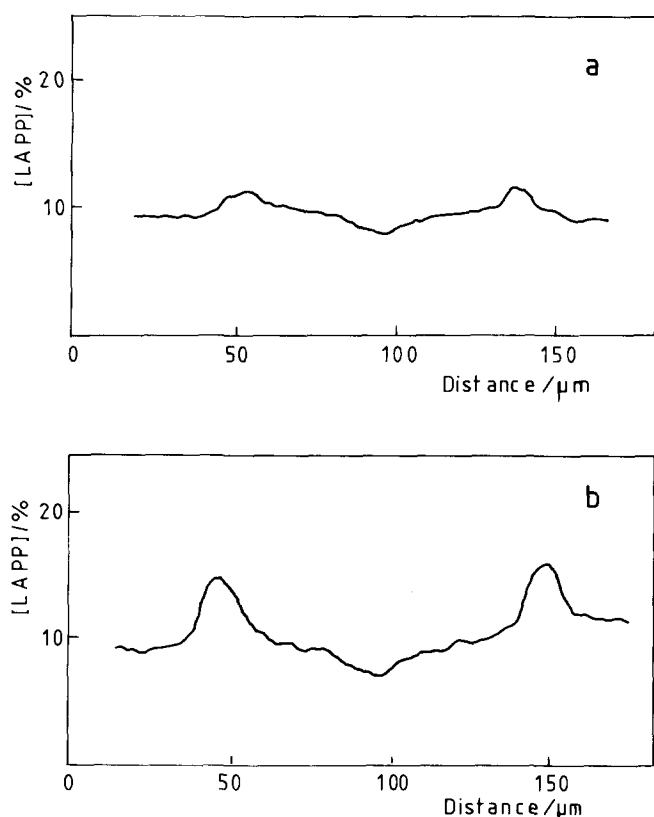


**Figure 3** Microdensitometer traces for fluorescence distribution across a single spherulite of IPP, in a sample containing 10% LAPP: (a) fully crystallized at 125°C; (b) fully crystallized at 135°C

the same methods to look at the distribution of APP in IPP, via the u.v. absorption or fluorescence of the labelled polymer.

Figure 2 is a fluorescence micrograph of a sample containing 10% LAPP in an IPP matrix, fully crystallized at 140°C and observed at room temperature. The bright fluorescence of the spherulite boundaries shows that the atactic polymer is rejected during crystallization and concentrates at the boundaries. At the same time, the spherulite centres are more crystalline and contain less atactic material, as shown by their dark centres. These distributions can be displayed as microdensitometer

traces and Figure 3 shows data typical of two crystallization temperatures. At the higher temperature, the peak in concentration at the spherulite boundaries and the dip in concentration at the centre are pronounced, indicating high crystallinity at the centre and high rejection of the atactic fraction. At the lower temperature, where crystallization is much more rapid, the profile becomes much flatter.

The concentration profile in any experiment was identical whether measured at room temperature or at the crystallization temperature. This is in marked contrast to low molecular weight additives, where redistribution occurs on cooling, as secondary crystallization occurs in the interlamellar regions<sup>13</sup>; it suggests that the APP is unable to redistribute in the spherulite during secondary crystallization.

Essentially identical results were obtained if the labelling was reversed and mixtures of APP with LIPP studied.

*Kinetics of redistribution.* We looked at the distribution of LAPP in partially crystallized IPP, either by direct observation at the crystallization temperature or by partial crystallization, quenching and observation at room temperature. Figure 4 shows a typical fluorescence micrograph, in which the concentration of fluorescer ahead of the growing spherulite-liquid interface, and the central dip, are clear. Variation in crystallization temperature showed the rejected peak profile becoming broader and increasing in height with increasing temperature of crystallization. Observations as a function of spherulite size (Table 2) show the peak concentration at the interface to be independent of spherulite size in the

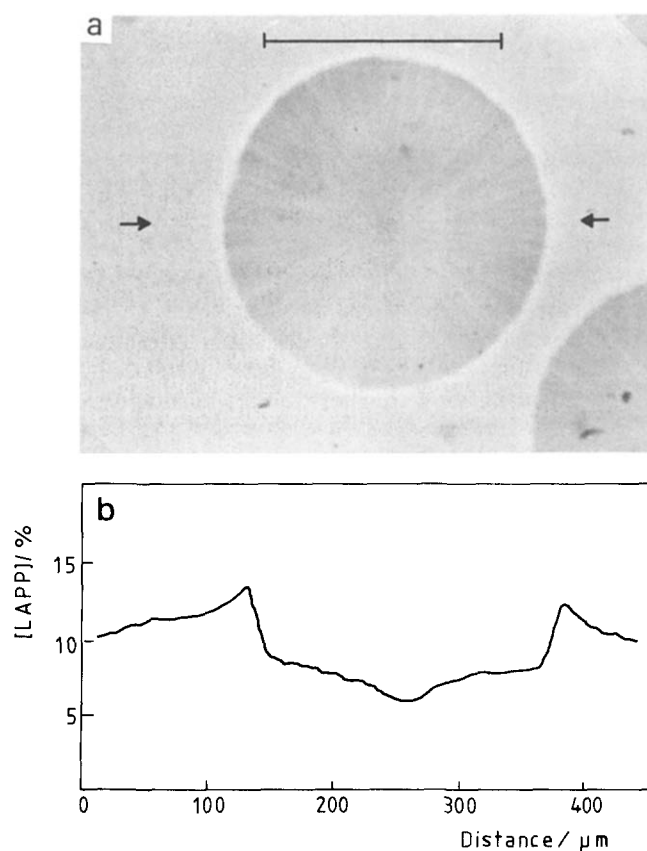


**Figure 4** (a) Fluorescence micrograph of a sample of IPP containing 10% LAPP. Sample was quenched after partial crystallization at 140°C and is viewed at room temperature. Scale bar, 200 μm. (b) Microdensitometer trace along line in (a) marked by arrows

**Table 2** Redistribution of atactic polymer during crystallization of IPP at 140°C<sup>a</sup>

Time (min)	Spherulite radius (μm)	Normalized centre concentration	Normalized peak concentration
240	160	0.727	1.125
300	210	0.706	1.106
360	240	0.683	1.150
420	275	0.666	1.166
480	325	0.566	1.170

<sup>a</sup> Measurements across a single spherulite during growth. Normalized to average concentration of fluorescer in the spherulite. Sample contained 10% of LAPP. Growth rate was 0.011 μm s<sup>-1</sup>

range 150–350 μm. Over the same range, the central dip in concentration becomes more distinct as the radius increases, presumably due to continuing crystallization at the spherulite centre.

The distribution profiles of APP in IPP represent the interaction of the crystallization kinetics with the diffusion of the atactic polymer within the spherulite and in the melt. A theoretical model for the kinetics of redistribution of small molecules during polymer crystallization has been derived by Calvert and Ryan<sup>12</sup> and is based upon zone-refining theory.

We assume that the molten polymer initially contains a uniform concentration of a single impurity unable to enter the crystal phase. We also assume that the interlamellar amorphous polymer in the growing spherulite, and the molten polymer, are identical and that mixing in the melt is diffusive. Partitioning between the spherulite and the melt can then be characterized by an interfacial partition coefficient  $K_1$  equal to the amorphous content of the spherulite at the interface. If the interface advances through the melt with constant growth rate and crystallinity, then rejection of impurity by the crystals will give a higher concentration at the interface and the excess impurity will diffuse away into the bulk melt at a rate determined by the diffusion coefficient in the melt and the concentration gradient. At the same time it may diffuse more slowly back into the spherulite.

If the impurity peak is broad compared with the average crystal thickness we can treat the spherulite as a uniform solid. The concentration profile of the impurity is then determined by the growth rate,  $K_1$ , (directly related to crystallinity) and the ratio of the diffusion coefficients  $D_S$  and  $D_L$  in the spherulite and the bulk liquid. The appropriate equations for spherical growth/rejection, in both two and three dimensions, have been formulated as a computer model<sup>12</sup>. Using this model for small probe molecules, with  $D_L$  as a variable, the spherulite growth rate measured in the microscope and a crystallinity measured by differential scanning calorimetry (d.s.c.), it was possible to get a good fit with measured concentration profiles over the entire range from the spherulite centre to the melt for typical spherulite sizes. Hence it was possible to estimate  $D_L$ .

To adapt this approach to APP in IPP, we crystallized samples containing up to 20% LAPP. Growth rates were measured in the hot-stage microscope and were independent of spherulite size. The growth rates were reduced by the atactic polymer although the effect was small for concentrations < 30%.  $K_1$  values were estimated from the primary crystallinities, calculated from heat of fusion measurements as a function of crystallization time, as described previously<sup>12</sup>. The primary crystallinity

decreased linearly with atactic content, suggesting that the atactic polymer is not incorporated into the crystallites to any significant extent.

Figure 5 is a typical example of an attempt to fit the observed concentration profile, in this case for a spherulite growing at 130°C. At this temperature  $D_S = 0.25 \mu\text{m}^2 \text{s}^{-1}$ , as measured by bulk diffusion, and the measured  $K_1 = 0.61$ . It is not possible to get a good fit over the whole of the curve and this is typical of our experience. With  $D_L = 4 \mu\text{m}^2 \text{s}^{-1}$  it is possible to get a good fit in the liquid region but the fit within the spherulite is very poor. The negative curvature of concentration within the spherulite is best fitted by a lower diffusion coefficient than that measured by bulk diffusion,  $\approx 0.05 \mu\text{m}^2 \text{s}^{-1}$ . The concentration step at the interface is clearly less than would be expected from the known crystallinity.

The step height at the spherulite boundary in the measured distribution corresponds to the  $K_1$ . Comparison with d.s.c. values (Table 3) shows observed values significantly higher than those from d.s.c., implying a higher atactic fraction in the polymer at the interface than predicted by d.s.c. For example, 30% atactic diluent at 135°C gives an observed  $K_1$  of 0.9, corresponding to only 10% crystallinity, whereas the calorimetric value is 36%.

We believe that the discrepancies between the simple theory and experiment arise because the atactic poly-

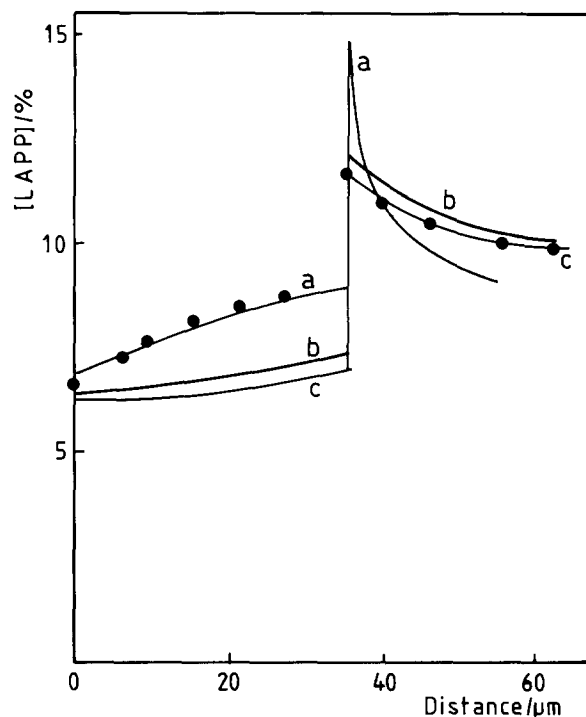


**Figure 5** Comparison of observed and computed LAPP distributions for a sample of IPP containing 10% LAPP, partially crystallized at 130°C.  $K_1 = 0.61$ . (a)  $D_S = 0.05 \mu\text{m}^2 \text{s}^{-1}$ ,  $D_L = 0.25 \mu\text{m}^2 \text{s}^{-1}$ ; (b)  $D_S = 0.25 \mu\text{m}^2 \text{s}^{-1}$ ,  $D_L = 1.25 \mu\text{m}^2 \text{s}^{-1}$ ; (c)  $D_S = 0.25 \mu\text{m}^2 \text{s}^{-1}$ ,  $D_L = 4.0 \mu\text{m}^2 \text{s}^{-1}$

**Table 3** Interfacial partition coefficients,  $K_1$ , from d.s.c. and u.v. measurements

	10 wt% LAPP			20 wt% LAPP		30 wt% LAPP	
	130°C	135°C	140°C	130°C	135°C	130°C	135°C
D.s.c.	0.61	0.58	0.58	0.63	0.61	0.67	0.64
U.v.	0.77	0.73	0.67	0.80	0.76	0.85	0.90

propylene is not rejected uniformly by the growing interface.

In a study of spherulite morphology using low molecular weight additives, Calvert and Ryan<sup>12</sup> found that spherulites observed at crystallization temperature appeared to be uniform but developed marked fibrosity on cooling, due to further reorganization on secondary recrystallization. The same is not true when the labelled material is APP. In this case the same fibrosity is seen in spherulites observed at either temperature. High concentrations of APP cause the spherulites to become very coarse, so that individual fibrils can be observed (Figure 6).

At high magnifications it can be seen that the growing spherulite usually has a fibrillar structure. The interface looks like a 'picket fence' with points at the tips of fibrils jutting forward into the melt. A small fraction of atactic material is rejected forwards by the tips of the fibrils, while most is trapped as the fibrils expand laterally towards one another. Hence  $K_1$  is close to 1, reflecting the low crystallinity in the region of the fibril tips. Unlike the small impurity molecules, the atactic polymer cannot enter the interlamellar regions but is restricted to the interfibrillar regions. The concentration of atactic polymer controls the development of fibrosity at high atactic

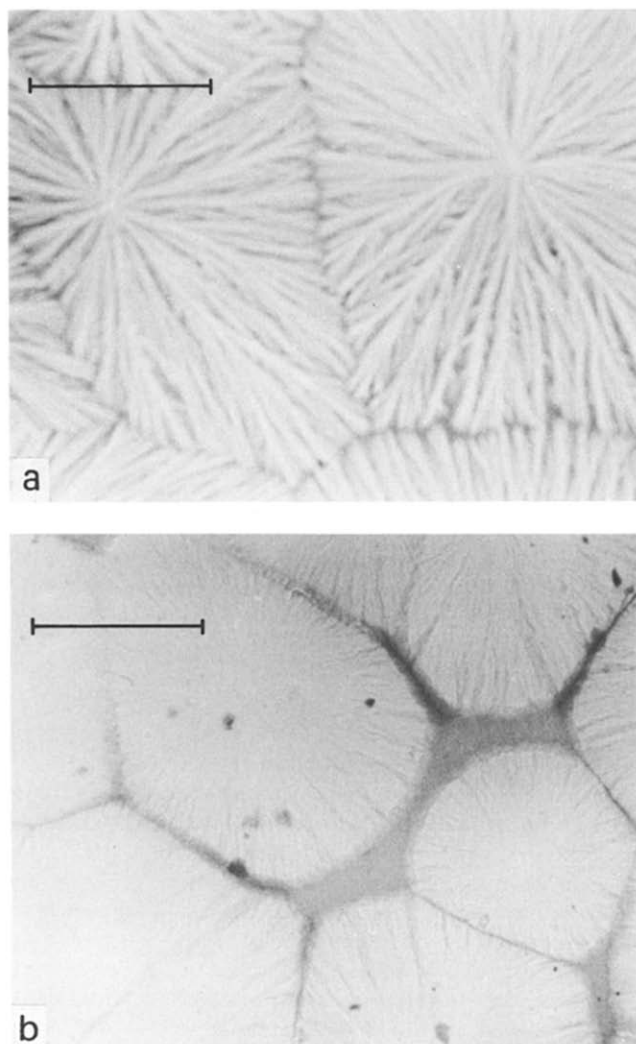


**Figure 6** Fluorescence micrographs of samples of LIPP containing unlabelled APP. Samples were crystallized fully at 125°C and are viewed at room temperature. Scale bars, 200  $\mu\text{m}$ . (a) 60% APP; (b) 40% APP

contents. This can be seen clearly in Figure 6, which compares fibrillar structures in labelled isotactic polypropylene crystallized with 40 and 60% of unlabelled atactic polymer.

The shape of the boundary peak is fairly insensitive to  $D_s$  and depends on  $D_L$ . It is possible to estimate  $D_L$  by fitting the boundary peak. Values of  $D_L$  in the range 1.5–3.5  $\mu\text{m}^2\text{s}^{-1}$  and a  $D_s$  of 0.05  $\mu\text{m}^2\text{s}^{-1}$  over the temperature range 130–140°C give the best fits. This value of  $D_s$  is considerably less than that derived above for diffusion into bulk solid polymer. This presumably reflects the difference between diffusion radially into a spherulite, in the growth studies, and diffusion which can also occur around spherulite boundaries in the low crystallinity zone.

## CONCLUSIONS

We have shown that the reaction of IPP with dansyl azide is a simple and convenient way of labelling the polymer so that it can be visualized in the optical microscope; this approach may have applications in other areas of polymer science, especially in the study of polymer mixing and interfaces.

Application of the u.v. or fluorescence microscope allows the diffusion of labelled polymer in bulk solid material to be measured and good fits to Fickian kinetics are obtained. In principle this approach could be extended to higher molecular weight diffusants.

Studies of rejection of atactic polymer during crystallization of isotactic material show that boundary rejection occurs but the kinetics are more complex than a simple model predicts. Apparently three types of amorphous material can be distinguished: interlamellar, interfibrillar and interspherulitic, with increasing accessibility to polymeric impurities. We have shown elsewhere<sup>20</sup> that concentration of atactic polymer at spherulite boundaries may have implications for oxidative stability of the polymer.

## ACKNOWLEDGEMENTS

We are grateful to ICI PLC for the supply of polypropylene and additives and to SERC for a grant to purchase the u.v. microscope. Thanks are also due to the Government of Turkey for their support for A.U.

## REFERENCES

- 1 Tirrell, M. *Rubber Chem. Technol.* 1984, **57**, 523
- 2 deGennes, P. *J. Chem. Phys.* 1984, **55**, 523
- 3 Klein, J. *Nature* 1978, **271**, 144
- 4 Mills, P. J., Green, P. F., Palmstrom, C. J., Majer, J. W. and Kramer, E. J. *Appl. Phys. Lett.* 1984, **45**, 957
- 5 Kunagi, Y., Watanabe, H., Miyasaka, K. and Hata, T. *J. Chem. Eng. Jpn* 1979, **12**, 1
- 6 Price, F. P., Gilmore, P. T., Thomas, E. L. and Laurence, R. L. *J. Polym. Sci., Symp.* 1978, **63**, 33
- 7 Gilmore, P. T., Falabella, F. and Laurence, R. L. *Macromolecules* 1980, **13**, 880
- 8 Bueche, F., Cashina, W. M. and Debye, P. *J. Chem. Phys.* 1952, **20**, 1956
- 9 Bueche, F. *J. Chem. Phys.* 1968, **48**, 6410
- 10 Billingham, N. C. and Calvert, P. D. *Pure Appl. Chem.* 1985, **57**, 1727
- 11 Billingham, N. C., Calvert, P. D. and Uzuner, A. *Eur. Polym. J.* 1989, **25**, 839
- 12 Calvert, P. D. and Ryan, T. G. *Polymer* 1978, **19**, 611

*Diffusion in polymers: N. C. Billingham et al.*

- |    |  |    |   |
|----|--|----|---|
| 13 | Calvert, P. D. and Ryan, T. G. <i>Polymer</i> 1982, <b>23</b> , 877; 1984, <b>25</b> , 921 | 17 | Crank, J. S. 'The Mathematics of Diffusion', Clarendon Press, Oxford, 1975                |
| 14 | Cantor, S. E. <i>A.C.S. Adv. Chem. Ser.</i> 1978, <b>169</b> , 253                         | 18 | Fleischer, G. <i>Polym. Bull.</i> 1983, <b>9</b> , 152; 1984, <b>11</b> , 75              |
| 15 | Billingham, N. C. and Calvert, P. D. <i>Dev. Polymer. Char.</i> 1982, <b>3</b> , 229       | 19 | Bachus, R. and Kimmiich, R. <i>Polymer</i> 1983, <b>24</b> , 964                          |
| 16 | Kissinger, J. B. and Hughes, R. E. <i>J. Phys. Chem.</i> 1959, <b>63</b> , 2002            | 20 | Knight, J. B., Calvert, P. D. and Billingham, N. C. <i>Polymer</i> 1985, <b>26</b> , 1713 |